Fusion Engineering and Design 139 (2019) 39–46

Contents lists available at ScienceDirect

Fusion Engineering and Design

journal homepage: www.elsevier.com/locate/fusengdes

Screw-based dynamics of a serial/parallel flexible manipulator for DEMO blanket remote handling

Stanislao Grazioso[a,*], Giuseppe Di Gironimo[a], Daniel Iglesias[b], Bruno Siciliano[a]

[a] CREATE/University of Naples Federico II, P.le Tecchio 80, 80125 Napoli, Italy
[b] RACE/UKAEA, Culham Science Centre, Abingdon, Oxfordshire OX14 3DB, UK

ARTICLE INFO

Keywords:
DEMO
Remote maintenance
Robot dynamics
Flexible manipulators
Tokamak

ABSTRACT

Remote handling of heavy in-vessel components inside nuclear fusion reactors requires the use of large robotic mechanisms, whose numerical analysis is highly complex. As a matter of fact, these robots are subject to large deformations, either induced by the geometric configuration of their mechanical structure or by the heavy payloads they usually transport. This work was motivated by the need of deriving physical-based predictive models able to simulate the mechanical behavior of such large robotic mechanisms, while performing dynamic tasks. The method formulates the dynamics of robotic manipulators on a Lie group, and uses a finite element procedure to discretize the flexible bodies. The method is applied to a complex mechanism, the serial/parallel flexible manipulator which has been recently selected for DEMO blanket remote handling. The case studies investigated in this paper involve the simulations of this manipulator while handling the inboard and outboard blanket segments according to the sequence of maneuvers planned for their removal processes from the vessel. The results show that such dynamic simulations could give useful information for design, analysis and control of remote handling equipment. The generality of the method makes this approach prone to be easily used in simulating the dynamics of other flexible manipulators for remote handling of large in-vessel components inside nuclear fusion reactors.

1. Introduction

The vertical maintenance system (VMS) for EU DEMO remote maintenance developes a concept for breeder blanket replacement via the upper ports at the top of the vacuum vessel (VV) [1]. The blanket handling procedure involves the use of robotic manipulators for the in-vessel operations and overhead cranes for the ex-vessel operations [2]. Typically, around 80 breeder blanket segments, each of ~12.5 m long and weighting up to 80 tonnes, will be contained into the vessel. Further, an ideal gap of 20 mm is required between two adiacent segments, in order to maximize tritium breeding and minimize neutron streaming [3]. Manipulating and handling such large components while maintaining tight clearances is highly challenging, since their motion often results in high levels of vibrations [4,5]. In order to predict and thus cancels these vibrations, methods able to simulate the nonlinear deformation of the in-vessel components and the large manipulators which are required to manouvre the components, in static and dynamic conditions, are highly required. This problem was indicated as one of the main issue in the current remote handling research for nuclear fusion [6].

Over the past years, many mathematical models have been introduced to simulate the dynamics of large flexible manipulators [7]. Currently, the most adopted approaches in the robotics research include lumped parameters models [8], assumed mode models [9], transfer matrix models [10]. They assume linear elasticity, small deflections, light damping and rotational motion of modest angular rate. Furthermore, they are usually suited only for serial manipulators with revolute joints [11]. Even if these are reasonable assumptions for most robotic devices, the nature of the movements for in-vessel operations, the mechanical complexity of the mechanisms involved, as well as the scale of the loads in a fusion scenario, push towards an alternative approach. We have tackled this problem by using a screw–based nonlinear finite element approach for flexible manipulators [12–14]. Finite element procedures provide several features of interest in this context: (i) modeling of manipulators with rigid/flexible elements; (ii) modeling of manipulators with all kind of joints, which can be either rigid or flexible; (iii) modeling of serial/parallel kinematic chain's topology using the same systematic approach. The finite element discretization process takes place within a modeling framework formulated on a Lie group, which uses the screw notations [15]. Then, the screw–based dynamic

* Corresponding author.
E-mail address: stanislao.grazioso@unina.it (S. Grazioso).

https://doi.org/10.1016/j.fusengdes.2018.12.029
Received 11 May 2018; Received in revised form 25 October 2018; Accepted 11 December 2018
0920-3796/ © 2018 EUROfusion Consortium. Published by Elsevier B.V. All rights reserved.

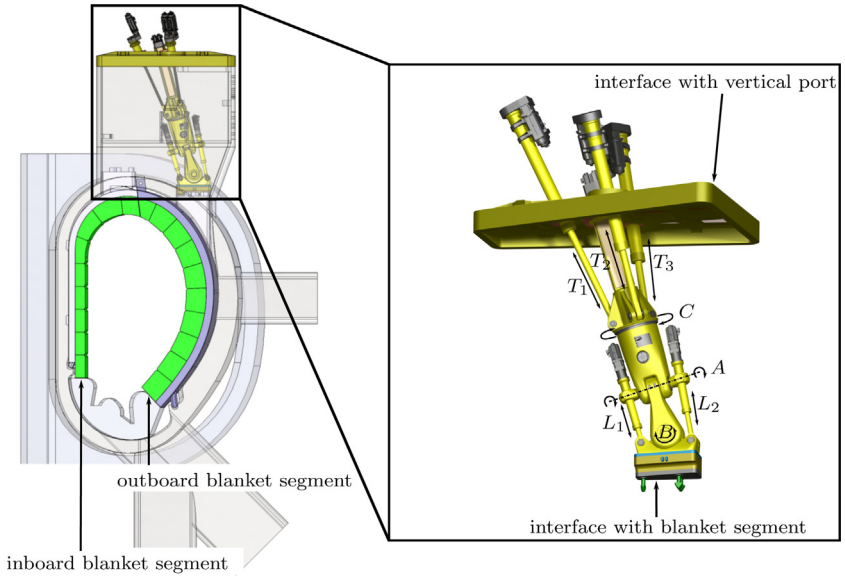

Fig. 1. Hybrid kinematic mechanism for EU DEMO blanket remote handling.

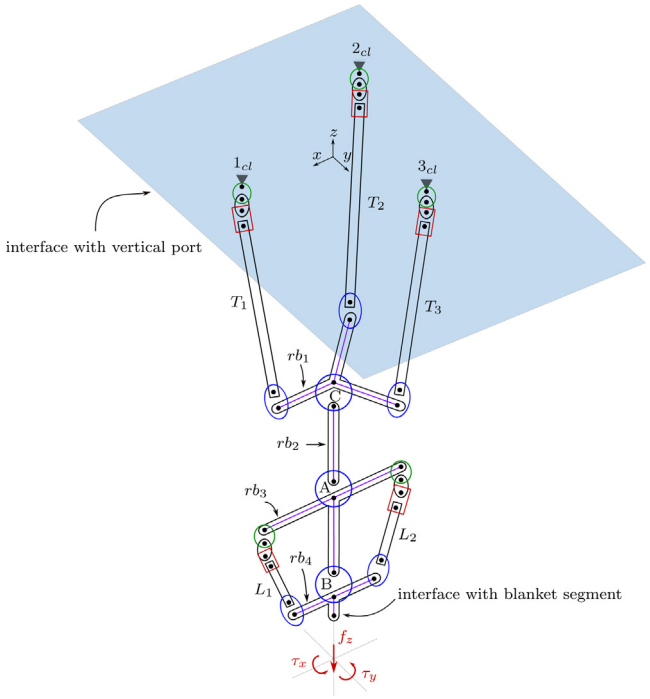

Fig. 2. Model of the hybrid kinematic mechanism.

Table 1
Point-to-point joint positions for the OBS removal. Linear measurements in [mm]; angular measurements in [deg].

	T_1	T_2	T_3	A	B	C
Home	3242.8	3242.8	3242.8	0	0	0
0	3032.8	2510.7	2814.7	−8.56	15.72	5.50
1	3003.5	2717.5	2742.7	−4.96	15.44	5.32
2	3032.8	2510.7	2814.7	−8.56	15.72	5.50
3	2891.6	2360.7	2674.4	−8.87	15.95	5.50
4	2839.4	2517.1	2393.9	5.52	14.89	5.45
5	2091.1	1763.3	1603.3	6.91	16.19	5.43
6	2437.4	2052.3	1899.5	7.17	23.29	4.80

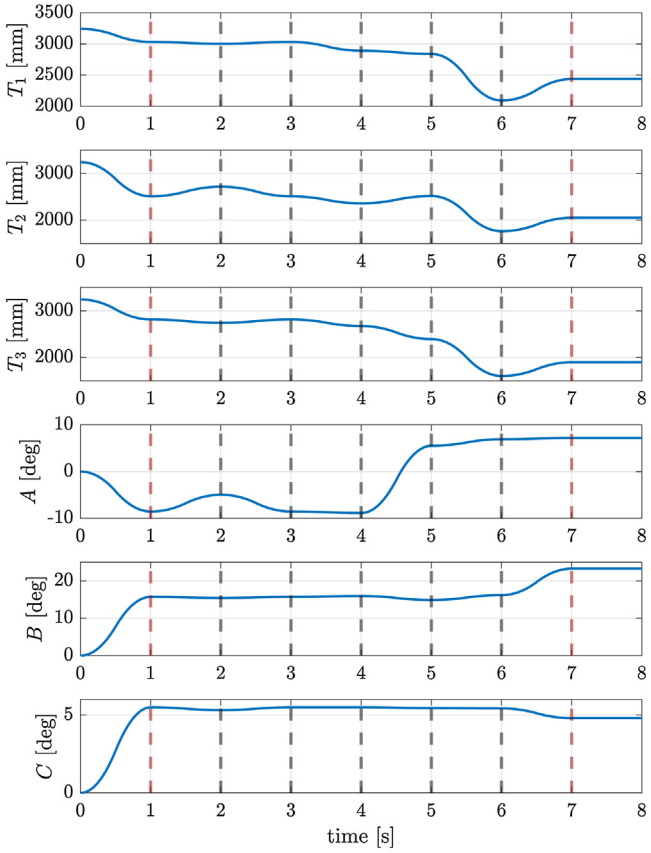

Fig. 3. Joint trajectories for the OBS removal.

model could be numerically solved by using geometric time integrators, which might significantly speed up the numerical computation of the equations of motion [16,17]. In this work, we apply this model for the dynamic simulation of the hybrid kinematic mechanism which has been recently proposed as the blanket transporter [18]. The main objective of this paper is to show how a general-purpose finite element mathematical formulation is promising towards modeling and simulation of manipulators for EU DEMO remote handling. In this context, dynamic models are essential for mechanical design, analysis of manipulator

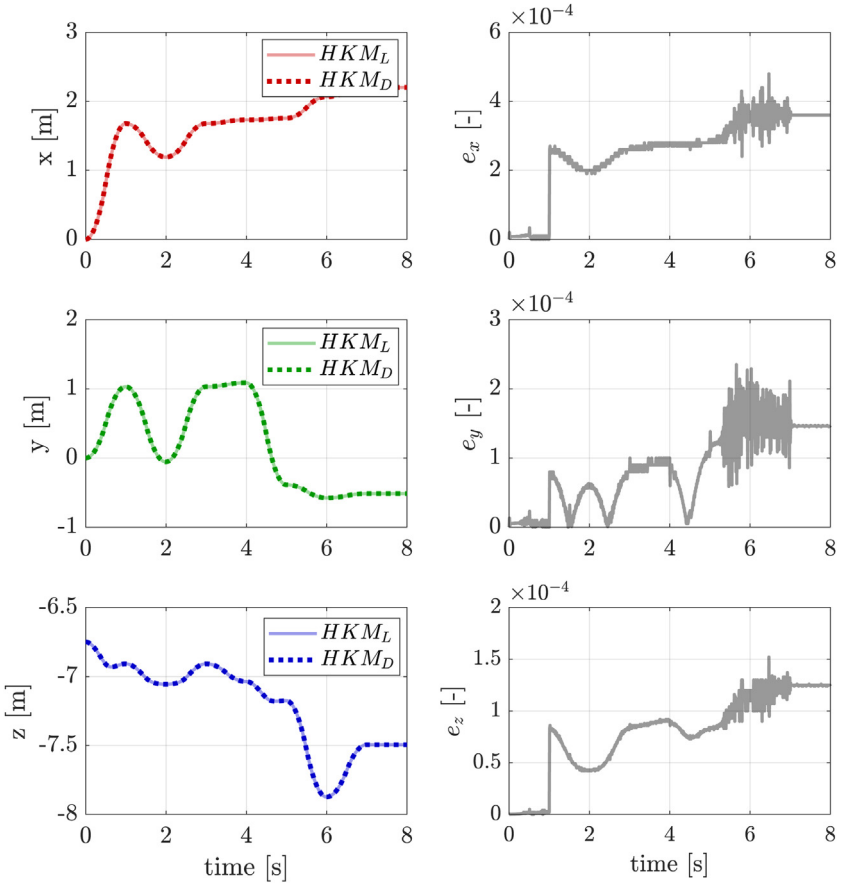

Fig. 4. Displacements of the tip of HKM in the test trajectory for the OBS removal. Solid line: HKM_L; Dotted line: HKM_D.

structures, design of model-based control algorithms, simulation of motion.

The rest of the paper is outlined as follows. In Section 2 we briefly describe the mechanics of the serial/parallel robotic manipulator. In Section 3 we derive its dynamic model, formulated on a Lie group. The dynamical simulations of the serial/parallel robotic manipulator during the blanket removal processes are addressed in Section 4. Finally, in Section 5 we discuss the conclusions of the current work and some possible future works.

2. Mechanics

The hybrid kinematic mechanism (HKM) illustrated in Fig. 1 is the recent system proposed for remote maintenance of breeder blanket segments for DEMO [18]. It allows the installation and replacement of the inboard and outboard blanket segments through the vertical upper port of the vessel. The HKM topology is hybrid, i.e. it includes a parallel and a serial kinematic structure. The parallel section comprises three linear actuators T_i which position the mechanism in space. The base of each actuator has a gimbal arrangement built into the port interface plate, while the other extremity of the actuator is linked with the mechanism through an hinge joint. The three revolute joints *A*, *B* and *C* in a serial configuration create an extended wrist. They respectively allow for a rotation about the axis *x*, *y* and *z*. The conceptual design of the HKM is fully described by Keep et al. in [18].

3. Dynamics

The screw-based formulation used in this work is based on *absolute variables* for the description of the large amplitude motions of the elements (rigid and flexible bodies), and *relative variables* for the description of the relative motions inside the joints. In the *SE*(3) formalism, these variables take the meaning of *frames*, which are:

- Nodal frames. A single rigid body is described by the motion of one node applied at its center of gravity, to which a local frame is attached. A flexible body is modeled as a discrete beam element composed by two extreme nodes, to which two local frames are attached and interpolated through an helical shape function [19]. For node *I*, we use the notation $\mathbf{H}_I$. These local frames belong to the *SE*(3) group; they have six degrees of freedom, namely three translations and three rotations, collected in a 4 × 4 matrix as

$$\mathbf{H}_I = \begin{bmatrix} \mathbf{R}_I & \mathbf{u}_I \\ \mathbf{0}_{1\times 3} & 1 \end{bmatrix} \tag{1}$$

  where $\mathbf{R}_I$ is a 3 × 3 rotation matrix and $\mathbf{u}_I$ is a 3 × 1 position vector, which define respectively the orientation and the position of the node with respect to a fixed inertial reference frame.
- Relative frames. If we consider two generic nodes $\mathbf{H}_1$ and $\mathbf{H}_2$ connected by a generic joint, the relative motion allowed by the joint *J* between the two nodes 1 and 2 can be described as

$$\mathbf{H}_2 = \mathbf{H}_1\mathbf{H}_{J,I} \tag{2}$$

  where $\mathbf{H}_{J,I}$ is a relative frame. These frames belong to a subgroup of *SE*(3); they have $k_J \leq 6$ degrees of freedom, depending on the joint [20].

The derivatives of the frames might be used to define the velocity and deformations of the bodies. Let us consider a scalar $a \in \mathbb{R}$; the derivatives of the nodal and relative frames $\mathbf{H}_I$ and $\mathbf{H}_{J,I}$ with respect to *a* can be written as

$$d_a(\mathbf{H}_I) = \mathbf{H}_I\tilde{\mathbf{a}}_I \tag{3}$$

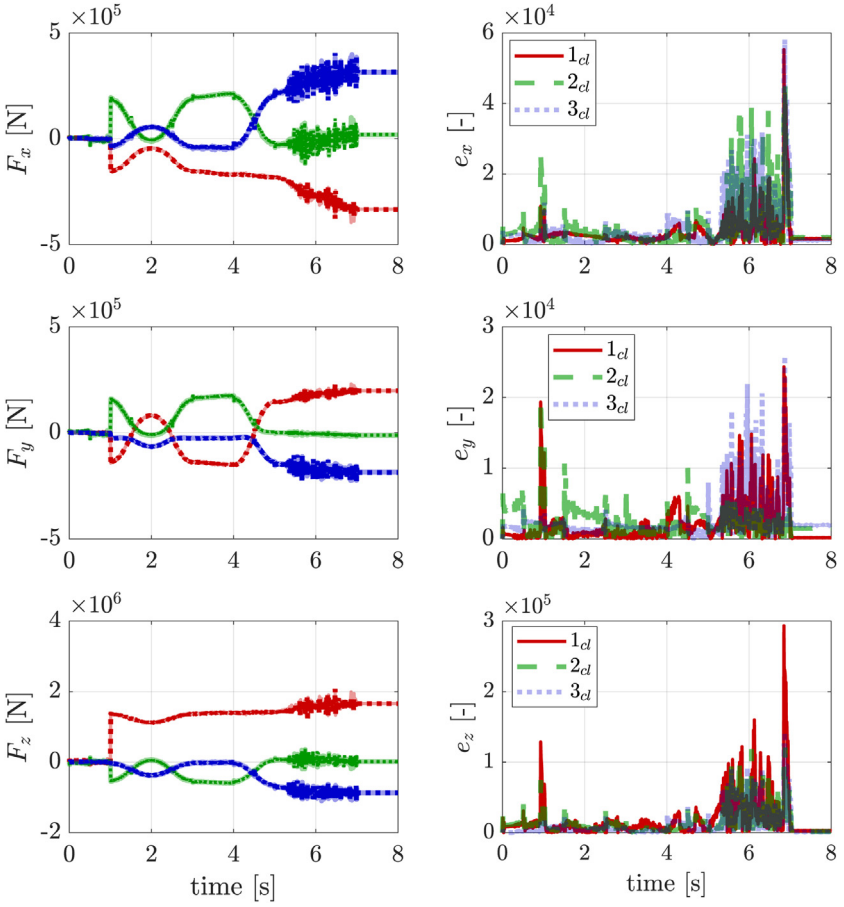

Fig. 5. Reaction forces of the HKM at the boundaries (interface with vertical port), during the test trajectory for the OBS removal. Red: 1_{cl}; Green: 2_{cl}; Blue: 3_{cl} (see Fig. 2). Solid line: HKM_L; Dotted line: HKM_D. (For interpretation of the references to color in text/this figure legend, the reader is referred to the web version of the article.).

Table 2
Point-to-point joint positions for the IBS removal. Linear measurements in [mm]; angular measurements in [deg].

	T_1	T_2	T_3	A	B	C
Home	3242.8	3242.8	3242.8	0	0	0
0	1433.5	2102.0	2006.6	5.78	−24.28	−5.14
1	1439.2	2058.5	1956.2	5.83	−21.16	−5.22
2	1433.6	2102.0	2006.6	5.78	−24.28	−5.14
3	1291.7	1978.1	1879.2	6.01	−25.04	−5.11
4	1411.4	1817.2	1725.1	4.69	−14.00	−5.47
5	2387.2	2357.4	2294.7	1.48	6.57	−5.59
6	2414.8	2249.4	2446.6	−7.28	5.91	−5.63
7	2175.1	1709.8	1944.9	−9.56	17.34	−5.42
8	2162.9	1720.8	1909.7	−8.02	17.47	−5.40
9	2183.2	1837.6	2008.2	−6.13	3.88	−5.64

$$d_a(\mathbf{H}_{J,I}) = \mathbf{H}_{J,I}\tilde{\mathbf{a}}_{J,I} = \mathbf{H}_{J,I}\widetilde{\mathbf{A}_J\mathbf{a}_{j,I}} \tag{4}$$

where $\tilde{\mathbf{a}}_I \in \mathfrak{se}(3)$. The element $\tilde{\mathbf{a}}_I$ is the Lie algebra associated to the Lie group $\mathbf{H}_I \in SE(3)$. In the screw theory, the Lie algebra $\tilde{\mathbf{a}}_I \in \mathfrak{se}(3)$ is called twist. It is composed by a positional part $\mathbf{v} = [v_1\, v_2\, v_3]^T \in \mathbb{R}^3$ and a rotational part $\boldsymbol{\omega} = [\omega_1\, \omega_2\, \omega_3]^T \in \mathbb{R}^3$ as

$$\tilde{\mathbf{a}}_I = \begin{bmatrix} 0 & -\omega_3 & \omega_2 & v_1 \\ \omega_3 & 0 & -\omega_1 & v_2 \\ -\omega_2 & \omega_1 & 0 & v_3 \\ 0 & 0 & 0 & 1 \end{bmatrix} \tag{5}$$

where in the up left 3×3 block of the matrix we can recognize the typical structure of the skew-symmetrix matrix associated with the rotational part of the twist.

The matrix $\mathbf{A}_J \in \mathbb{R}^{6\times kJ}$ in (4) spans the subspace of the allowed relative motions foreseen by the joint, while $\mathbf{a}_{J,I} \in \mathbb{R}^{kj}$ in (4) is a custom vector depending on the joint. For example, for a revolute joint, $\mathbf{A}_J$ reduces to a six–dimensional vector and $\mathbf{a}_{J,I}$ reduces to a scalar as

$$\mathbf{A}_{J,r} = \begin{bmatrix} \mathbf{0}_{3x1} \\ \mathbf{n}_r \end{bmatrix}; \quad \mathbf{a}_{j,I,r} = a_r \tag{6}$$

where $\mathbf{n}_r \in \mathbb{R}^3$ is the axis of the joint and $a_r \in \mathbb{R}$ is the derivative of the rotation angle. Indeed, for a prismatic joint we have

$$\mathbf{A}_{J,p} = \begin{bmatrix} \mathbf{n}_p \\ \mathbf{0}_{3\times1} \end{bmatrix}; \quad \mathbf{a}_{j,I,p} = a_p \tag{7}$$

where $\mathbf{n}_p \in \mathbb{R}^3$ is the axis of the joint and $a_p \in \mathbb{R}$ is the derivative of the axial displacement.

The equations of motion of a flexible robotic manipulator based on the screw-theory have been presented in [12]. In the rest of this section, we underline the main aspects which have led to the development of the dynamic model of the HKM.

3.1. Equations of motion

The equations of motion of a flexible manipulator composed by n nodes and m joints can be written as differential-algebraic equations (DAE) formulated on a Lie group as

$$\dot{\mathbf{H}} = \mathbf{H}\widetilde{\mathbf{A}\boldsymbol{\eta}} \tag{8}$$

$$\mathbf{f}_{\text{ine}}(\mathbf{H}, \boldsymbol{\eta}, \dot{\boldsymbol{\eta}}) + \mathbf{f}_{\text{int}}(\mathbf{H}) + \mathbf{f}_{\varphi}(\mathbf{H}, \boldsymbol{\lambda}) = \mathbf{f}_{\text{ext}}(\mathbf{H}) \tag{9}$$

$$\boldsymbol{\varphi}(\mathbf{H}) = \mathbf{0} \tag{10}$$

The kinematic equations (8) involve the time derivative of the element $\mathbf{H}$, which collects the motion variable of the manipulator as

$$\mathbf{H} = \text{diag}(\mathbf{H}_1, \ ..., \mathbf{H}_n, \ \mathbf{H}_{J,1}, \ ..., \mathbf{H}_{J,m}) \tag{11}$$

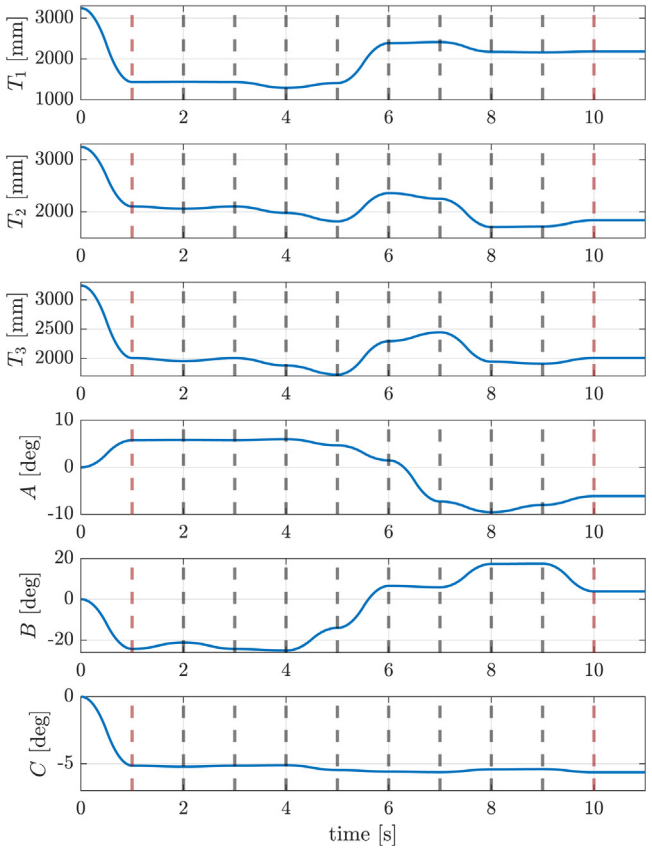

Fig. 6. Joint trajectories for the IBS removal.

where $\mathbf{H}_I$, $I = 1, \ldots, n$ denotes a nodal frame, while $\mathbf{H}_{J,I}$, $I = 1, \ldots, m$ denotes a relative frame. The element (11) can be interpreted as an element of a $(6n + 6m)$-dimensional Lie group. The velocity vector $\boldsymbol{\eta} \in \mathbb{R}^{6n+6m}$ is given by

$$\boldsymbol{\eta} = \left[\boldsymbol{\eta}_1^T \ldots \boldsymbol{\eta}_n^T \boldsymbol{\eta}_{J,1}^T \ldots \boldsymbol{\eta}_{J,m}^T \right]^T \tag{12}$$

where $\boldsymbol{\eta}_I \in \mathbb{R}^6$ denotes the absolute velocity vector of each node, while $\boldsymbol{\eta}_{J,I} \in \mathbb{R}^6$ is the relative velocity vector of each joint. These vectors comes up respectively from (3) and (4), where the scalar a is represented by the time variable t. The joint matrix $\mathbf{A} \in \mathbb{R}^{(6n+6m)\times(6m+k)}$ is given by

$$\mathbf{A} = \text{diag}(\mathbf{I}_{6\times6}, \ldots, \mathbf{I}_{6\times6}, \mathbf{A}_1, \ldots, \mathbf{A}_m) \tag{13}$$

where n denotes the number of nodes, m the number of joints, $k = k_1 + \ldots + k_m$ the degrees of freedom of all joints (each joint has k_J degrees of freedom). It includes the matrices $\mathbf{A}_J$ whose expression depends on the particular joint involved in the model (for a revolute joint, see (6), for a prismatic joint, see (7)).

The dynamic equations (9) include the discretized global inertia forces $\mathbf{f}_{ine}$, the discretized global internal forces $\mathbf{f}_{int}$, the discretized constraint forces $\mathbf{f}_{\phi}$ and the discretized global external forces $\mathbf{f}_{ext}$. The internal forces include the elastic forces of the beams and the elastic forces of the joints. Indeed, an elastic joint can be modeled as a spring element inside the joint: the presence of a spring element I add to the internal forces the contribution given by $\mathbf{f}_{int,I}(\boldsymbol{\delta}_I) = \mathbf{K}_I\boldsymbol{\delta}_I$, where $\mathbf{K}_I = \text{diag}(K_{I,1}, \ldots K_{I,k_J})$ is the diagonal stiffness matrix and $\boldsymbol{\delta}_I$ is the internal deflection of the joint. The constraint forces, using the Lagrange multiplier method, can be expressed as $\mathbf{f}_{\boldsymbol{\varphi}}(\mathbf{H}, \boldsymbol{\lambda}) = \mathbf{A}^T\boldsymbol{\varphi}_q(\mathbf{H})\boldsymbol{\lambda}$, being $\boldsymbol{\varphi}_q$ the gradient of the constraint (10) and $\boldsymbol{\lambda}$ the Lagrange multiplier vector associated with the constraint (10).

The kinematic constraint equations (10) involve six constraints for each joint. These equations basically state which are the direction of allowed motion, according to the joints included into the model.

Finally, the DAE system (8)–(10) must be solved for $(\mathbf{H}, \boldsymbol{\lambda})$. To this end, several numerical solution methods exist from the literature; particularly appealing are the implicit geometric time integration schemes for the prediction phase and Newton–Raphson iterative procedures for the correction phase [21].

3.2. Description of the HKM dynamic model

The model of the HKM is illustrated in Fig. 2. It comprises four rigid bodies (rb_i, $i = 1, \ldots, 4$), five universal joints (green circles), five prismatic joints (red rectangles), five hinges and three revolute joints (blue circles). The inertia properties of the rigid bodies (mass and rotation inertia) have been estimated from the CAD model of the manipulator.

We use two strategies to account for flexibility in the linear actuators. The first one follows a lumped approach, by modeling the linear actuator as a longitudinal system with point mass-spring behaviour. The spring stiffness was calculated based on the cross-section area of the actuator and Young's modulus, by considering structural steel as material. The HKM modeled with this approach will be indicated in the following as HKM_L. The second strategy follows a distributed approach, by modeling the linear actuator with one nonlinear beam where the only finite stiffness is the axial one, which has been computed again using the cross-section area of the actuator and Young's modulus, by considering structural steel as material. The HKM modeled with this approach will be indicated in the following as HKM_D.

The objective of the HKM is to safely handle an heavy payload, namely the breeder blanket. In a first investigation, we consider the breeder blanket as a point mass applied in its center of gravity (CoG). Thus, its influence on the HKM is equivalent to a force f_z downward z-axis, whose intensity is given by the weight force of the breeder blanket, plus two torques τ_x and τ_y about the x and y axes whose intensity is given by the product of the weight force and the distance between the CoG and the interface with blanket segment, respectively computed along the y and x axes. The value of the forces and moments applied at at the interface with blanket segments are given in the next section.

4. Simulations and results

The case study simulates the dynamics of the HKM while performing the sequence of maneuvers which have been planned for the removal of the outboard blanket segment (OBS) and inboard blanket segment (IBS). The two sequences of maneuvers translate into two sequences of point-to-point motions. Each joint of the manipulator moves from an initial to a final configuration through a sequence of points so as to guarantee a correct blanket removal. In particular, for the OBS removal, six maneuvers have been planned; for the IBS removal, nine maneuvers have been planned [22]. In order to generate a joint motion trajectory which can interpolate the sequences of point-to-point joint configuration, a trajectory planning algorithm must be formulated. As a first investigation, we suppose a bang-bang acceleration profile, with 0.5 s of positive acceleration followed by 0.5 s of negative acceleration, to reach each of the desired joint configuration. The bang-bang acceleration profile translates into the triangular profile at the velocity level, and the parabolic-parabolic profile (the S-shape) at the position level. The acceleration value for each point-to-point sequence has been computed as $\ddot{q} = 4(q_f - q_i)/t_f^2$, where q_i is the initial position of the manouvre, q_f the final position of the manouvre, t_f the time duration of each manouvre, in this test case 1 s. The loads applied at the tip for simulating the blanket will be given for the OBS and IBS removal processes. In the following, for the two sequences, the displacements of the tip of the robotic manipulator, as well as the reaction forces at the boundaries, i.e. at the interface with the vertical port, for the two developed models, HKM_L and HKM_D are given. Further, we also report an error measuring the distance between the two models, given by

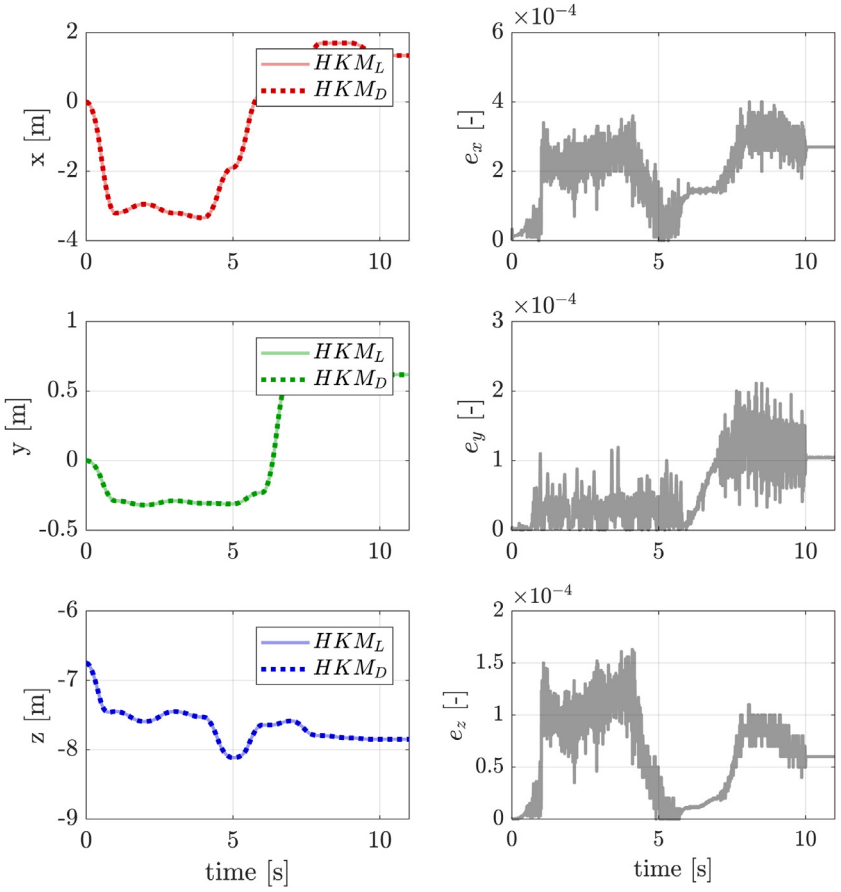

Fig. 7. Displacements of the tip of HKM in the test trajectory for the IBS removal. Solid line: HKM_L; Dotted line: HKM_D.

$$e = \text{abs}(v_{\text{HKM},L} - v_{\text{HKM},D}) \tag{14}$$

where v indicates the displacement or force values.

4.1. Removal of the outboard blanket segment

The removal of the outboard blanket segment involves six maneuvers, given in Table 1. In this table, we also include the home configuration of the manipulator, as well as the initial configuration of the OBS removal sequence (indicated with 0). The resulting *S*-shaped joint trajectories are illustrated in Fig. 3. The loads applied at the tip of HKM are: $f_z = -748\,800$ N, $\tau_x = 388\,100$ N m and $\tau_y = 290\,200$ N m. Notice that these loads are applied when the HKM reaches the initial configuration 0, at $t = 1$ s. Indeed, the trajectory from the home configuration to the initial configuration allows configurating the mechanism into the starting position of the sequence; thus, in this manouvre there is no blanket at the interface. Fig. 4 records the displacements of the tip of the manipulator in the trajectory corresponding to the OBS removal, for the two models HKM_L and HKM_D. As we can appreciate from the plots, the two models give similar results; the relatively small error is due to the high frequency induced by the flexible elements in the distributed model. Fig. 5 reports the reaction forces at the boundaries of the model, namely at the nodes 1_{cl}, 2_{cl} and 3_{cl}. We can see that the reaction forces assume relatively small values till 1 s, when the manipulator moves without the payload. After, the reaction forces suddenly rise. Further, for each point-to-point motion of 1 s duration, we can see an increase of the forces at half of this duration, which correspond to the change of curvature of the joint positional motion. The trajectory for the OBS removal is critical for the mechanical structure after 5 s, since between 5 and 6 s the linear actuators suddenly change their excursions from the 4th to the 5th configuration. A possible solution is to spread this manouvre into a larger time duration. The HKM_L and HKM_D models seem to give almost identical results regarding the reaction forces; however, as we can see from the error plots, the differences reach values in the order of 10^4. This value seems huge, but it is one order of magnitude less than the values of the forces. Even if part of this error is due to the high frequency induced by the flexible elements in the distributed model, we can state that there could be a substantial difference in estimating the reaction forces with less realistic models.

4.2. Removal of the inboard blanket segment

The removal of the inboard blanket segment involves nine maneuvers, given in Table 2. As before, we also include the home configuration of the manipulator, as well as the initial configuration of the IBS sequence (indicated with 0). The resulting *S*-shaped joint trajectories are illustrated in Fig. 6. The loads applied at the tip of HKM are: $f_z = -588\,600$ N, $\tau_x = -256\,900$ N m and $\tau_y = 682\,100$ N m. Again, these loads are applied when the HKM reaches the initial configuration 0, at $t = 1$s. Indeed, the trajectory from the home configuration to the initial configuration allows configurating the mechanism into the starting position of the sequence, without the presence of the blanket at the interface. Fig. 7 records the displacements of the tip of the manipulator in the test trajectory for the IBS removal, for the two models HKM_L and HKM_D. A close agremeent of the two models is observed again; the relatively small error is due to the high frequency induced by the flexible elements in the distributed model. Regarding the reaction forces at the boundaries (see Fig. 8), in this case we can notice even a worst condition for the mechanical structure at the interface. Indeed, in this case, from the beginning (from the home to the initial configuration) we have a larger excursion for the linear actuators and the revolute joints, as we can see from Fig. 6. A possible solution to mitigate this behavior is to spread the initial manouvre into a larger duration.

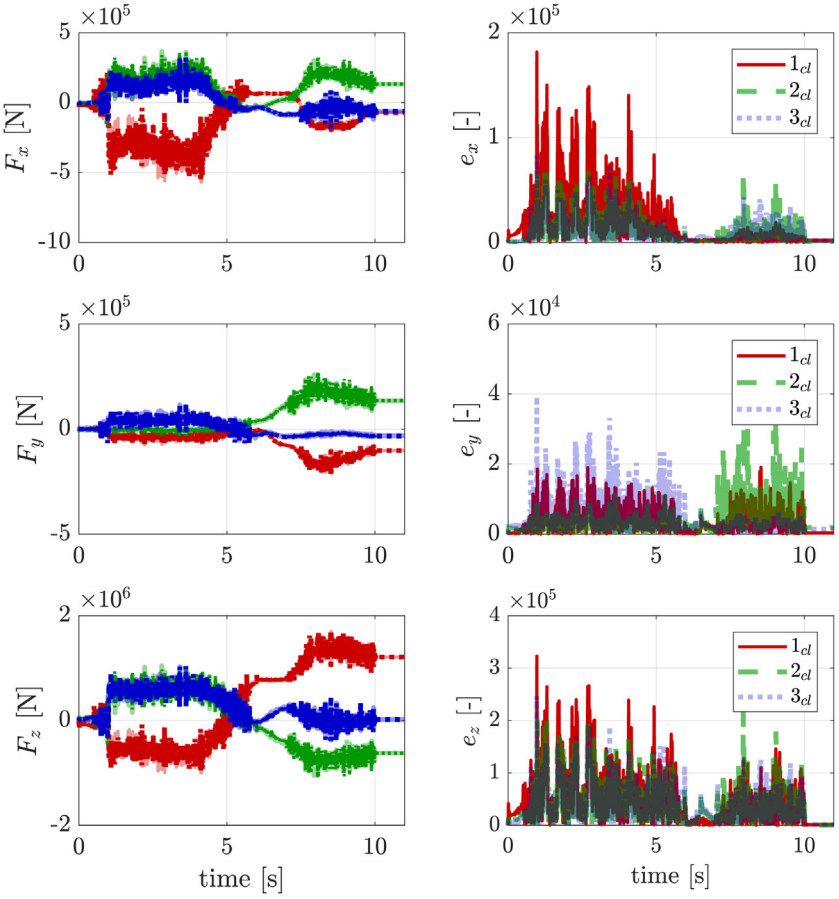

Fig. 8. Reaction forces of the HKM at the boundaries (interface with vertical port), during the test trajectory for the OBS removal. Red: 1_{cl}; Green: 2_{cl}; Blue: 3_{cl} (see Fig. 2). Solid line: HKM_L; Dotted line: HKM_D. (For interpretation of the references to color in text/this figure legend, the reader is referred to the web version of the article.).

For the errors, the discussion made for the OBS removal, is valid also for the IBS removal.

5. Conclusions

In this paper we proposed the use of a screw-based dynamic model to simulate the mechanical behavior of flexible manipulators used for remote handling procedures. We have shown the feasibility of the approach by simulating the HKM while handling the outboard and inboard blanket segment according to the sequence of maneuvers which have been planned for their removal process. We have selected a test joint trajectory algorithm and we have simulated the displacements of the manipulator tip as well as the reaction forces at the boundaries, as resulted from the simulations using two modeling assumptions.

Dynamic models could play an important role in providing information for the mechanical and control design. Further, they allow simulating the motion of mechanical systems during remote tasks.

In challenging domains as fusion reactors vessels, where remote handling procedures involve the manipulation/transportation of large payloads in tiny spaces, it is crucial to have realistic virtual models based on computational mechanics strategies, which can help in planning safe operations, in combination to full-scale physical mock up.

Acknowledgements

This work has been carried out within the framework of the EUROfusion Consortium and has received funding from the Euratom research and training program 2014-2018 under grant agreement No 633053. In particular, this work was developed during the the FlexARM project (http://www.flexarm-project.eu/), which has received funding under the EUROfusion Engineering Grant EEG-2015/21 *"Design of Control Systems for Remote Handling of Large Components"*. The views and options expressed herein do not necessarily re ect those of the European Commision.

References

[1] A. Loving, O. Crofts, N. Sykes, D. Iglesias, M. Coleman, J. Thomas, J. Harman, U. Fischer, J. Sanz, M. Siuko, et al., Pre-conceptual design assessment of demo remote maintenance, Fusion Eng. Des. 89 (9) (2014) 2246–2250, https://doi.org/10.1016/j.fusengdes.2014.04.082.

[2] M. Coleman, N. Sykes, D. Cooper, D. Iglesias, R. Bastow, A. Loving, J. Harman, Concept for a vertical maintenance remote handling system for multi module blanket segments in demo, Fusion Eng. Des. 89 (9) (2014) 2347–2351, https://doi.org/10.1016/j.fusengdes.2014.02.047.

[3] O. Crofts, A. Loving, D. Iglesias, M. Coleman, M. Siuko, M. Mittwollen, V. Queral, A. Vale, E. Villedieu, Overview of progress on the European demo remote maintenance strategy, Fusion Eng. Des. 109 (2016) 1392–1398, https://doi.org/10.1016/j.fusengdes.2015.12.013.

[4] S. Grazioso, G. Di Gironimo, W. Singhose, B. Siciliano, Input predictive shaping for vibration control of flexible systems, 2017 IEEE Conference on Control Technology and Applications (CCTA), IEEE (2017) 305–310, https://doi.org/10.1109/CCTA.2017.8062480.

[5] S. Grazioso, G. Di Gironimo, On the use of robust command shaping for vibration reduction during remote handling of large components in tokamak devices, 2018 26th International Conference on Nuclear Engineering, ASME (2018) https://doi.org/10.1115/ICONE26-82346.

[6] R. Buckingham, A. Loving, Remote-handling challenges in fusion research and beyond, Nat. Phys. 12 (5) (2016) 391–393, https://doi.org/10.1038/nphys3755.

[7] A. De Luca, W.J. Book, Robots with flexible elements, Springer Handbook of Robotics, Springer, 2016, pp. 243–282.

[8] W. Khalil, M. Gautier, Modeling of mechanical systems with lumped elasticity, 2000 IEEE International Conference on Robotics and Automation, Vol. 4, IEEE (2000) 3964–3969, https://doi.org/10.1109/ROBOT.2000.845349.

[9] R.H. Cannon Jr., E. Schmitz, Initial experiments on the end-point control of a flexible one-link robot, Int. J. Robot. Res. 3 (3) (1984) 62–75.

[10] R.W. Krauss, W.J. Book, Transfer matrix modeling of systems with noncollocated feedback, J. Dyn. Syst. Meas. Control 132 (6) (2010) 061301.

[11] W.J. Book, Recursive lagrangian dynamics of flexible manipulator arms, Int. J. Robot. Res. 3 (3) (1984) 87–101.

[12] S. Grazioso, V. Sonneville, G. Di Gironimo, O. Bauchau, B. Siciliano, A nonlinear finite element formalism for modelling flexible and soft manipulators, IEEE

International Conference on Simulation, Modeling, and Programming for Autonomous Robots (SIMPAR), IEEE (2016) 185–190, https://doi.org/10.1109/SIMPAR.2016.7862394.
[13] S. Grazioso, G. Di Gironimo, B. Siciliano, Analytic solutions for the static equilibrium configurations of externally loaded cantilever soft robotic arms, 2018 IEEE International Conference on Soft Robotics (RoboSoft), IEEE (2018) 140–145, https://doi.org/10.1109/ROBOSOFT.2018.8404910.
[14] S. Grazioso, G. Di Gironimo, B. Siciliano, A geometrically exact model for soft continuum robots: The finite element deformation space formulation, Soft Robot. (2018), https://doi.org/10.1089/soro.2018.0047.
[15] R. Ball, A treatise on the theory of screws, (1900) (1900 (Reprinted 1998)).
[16] O. Brüls, A. Cardona, On the use of lie group time integrators in multibody dynamics, J. Comput. Nonlinear Dyn. 5 (3) (2010) 031002.
[17] O. Brüls, A. Cardona, M. Arnold, Lie group generalized-α time integration of constrained flexible multibody systems, Mech. Mach. Theory 48 (2012) 121–137, https://doi.org/10.1016/j.mechmachtheory.2011.07.017.
[18] J. Keep, S. Wood, N. Gupta, M. Coleman, A. Loving, Remote handling of demo breeder blanket segments: blanket transporter conceptual studies, Fusion Eng. Des. (2017).
[19] S. Grazioso, G. Di Gironimo, B. Siciliano, From differential geometry of curves to helical kinematics of continuum robots using exponential mapping, Advances in Robot Kinematics 2018, Springer International Publishing, Cham, 2019, pp. 319–326, https://doi.org/10.1007/978-3-319-93188-3_37.
[20] V. Sonneville, O. Brüls, A formulation on the special Euclidean group for dynamic analysis of multibody systems, J. Comput. Nonlinear Dyn. 9 (4) (2014) 041002.
[21] O. Brüls, A. Cardona, M. Arnold, Lie group generalized-α time integration of constrained flexible multibody systems, Mech. Mach. Theory 48 (2012) 121–137.
[22] J. Keep, S. Wood, N. Gupta, Concept design description for blanket transporter, EFDA_D_2MRZLG, (2018).